GAPDH mRNA. PCR-amplified products were also electrophoresed on 2% agarose gels to confirm that single bands were amplified.

In Vitro Matrigel Assay

HUVECs (1×10^5 cells) were seeded onto 24-well plates coated with Matrigel (Becton Dickinson) in the presence of the combination of control buffer, AM (10^{-7} mol/L), VEGF (10 ng/mL), or neutralizing antibodies against KDR (2 μg/mL, R&D Systems). After incubation for 18 hours, tube formation area was measured as described previously.[17] The control was defined as 100% tube formation, and the percent increase was calculated for each sample.

Measurements of Cytokines

A total of 1×10^6 MNCs or HUVECs were plated in serum-free medium with or without AM (10^{-7} mol/L) on 12-well plates. After 24-hour incubation, the conditioned medium was collected, and VEGF, basic fibroblast growth factor, and hepatocyte growth factor were measured with enzyme immunoassay kits (R&D Systems).

Migration Assay

Migration assay of smooth muscle cells (SMCs) was performed with Transwell (Coster) 24-well plates composed of a collagen-coated membrane with 8-μm pores. Human aortic SMCs, preincubated with serum-free medium for 24 hours to maintain quiescence, were seeded on the upper chamber at a concentration of 1×10^6 cells/mL. Serum-free medium containing control buffer, AM (10^{-7} mol/L), or AM plus wortmannin (50 nmol/L) was placed in the lower chamber. After incubation for 12 hours, the number of migrated cells was counted in the randomly selected fields (n=5).

Statistical Analysis

All values are expressed as mean±SEM. Student's unpaired *t* test was used to compare differences between 2 groups. Comparisons of parameters among 3 or 4 groups were made by 1-way ANOVA, followed by Scheffé multiple comparison test. Comparisons of the time course of the LDPI index were made by 2-way ANOVA for repeated measures, followed by Scheffé multiple comparison tests. A probability value <0.05 was considered statistically significant.

Results

Blood Perfusion and Capillary Density

Blood perfusion of the ischemic hindlimb increased modestly but gradually in the AM and MNC groups after treatment (Figure 1A). Interestingly, blood perfusion in the AM+MNC group markedly improved within 2 weeks after treatment and showed further improvement thereafter. The LDPI index was significantly higher in the AM, MNC, and AM+MNC groups than in the control group 3 weeks after surgery (Figure 1B). Importantly, the LDPI index was highest in the AM+MNC group among the 4 groups.

Alkaline phosphatase staining of ischemic muscle showed significant augmentation of neovascularization in the AM, MNC, and AM+MNC groups (Figure 2A). The capillary/muscle fiber ratio of ischemic muscle was highest in the AM+MNC group, followed by the MNC group, AM group, and control group (Figure 2B).

Differentiation of Transplanted MNCs

Three weeks after MNC transplantation, PKH26-labeled MNCs were frequently observed in the AM+MNC group, and these transplanted cells were positive for vWF (Figure 3A). Most of these cells were also stained by CD31 (data not shown). The number of PKH26/vWF double-positive cells was significantly higher in the AM+MNC group than in the

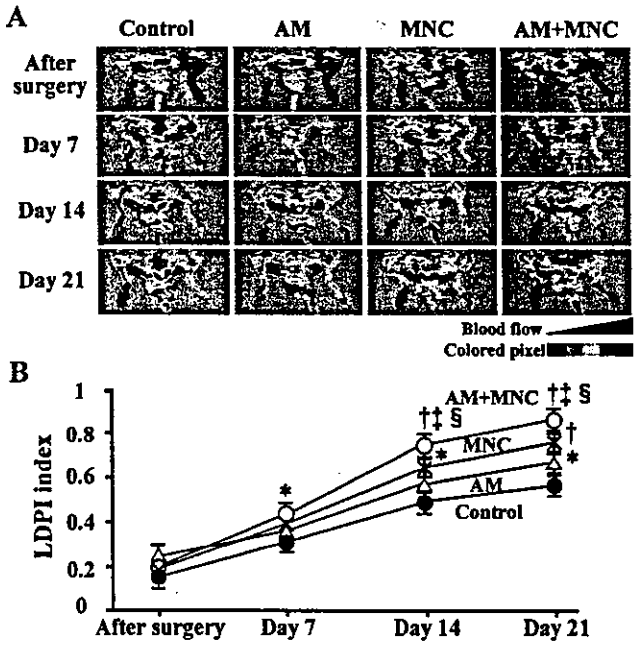

Figure 1. A, Representative examples of serial laser Doppler perfusion images. Blood perfusion of ischemic hindlimb increased notably in AM+MNC group (red to yellow). B, Quantitative analysis of hindlimb blood perfusion with LDPI index, ratio of ischemic to nonischemic hindlimb blood perfusion. Data are mean±SEM. *$P<0.05$ and †$P<0.01$ vs control; ‡$P<0.01$ vs AM; §$P<0.05$ vs MNC.

MNC group (Figure 3B). Although PKH26/α-SMA double-positive cells were not detected in ischemic muscle of each group, newly formed vascular structures in the AM+MNC group included α-SMA–positive cells (Figure 3C). The number of α-SMA–positive cells in the MNC-derived vascular structures was significantly higher in the AM+MNC group than in the MNC group (Figure 3D).

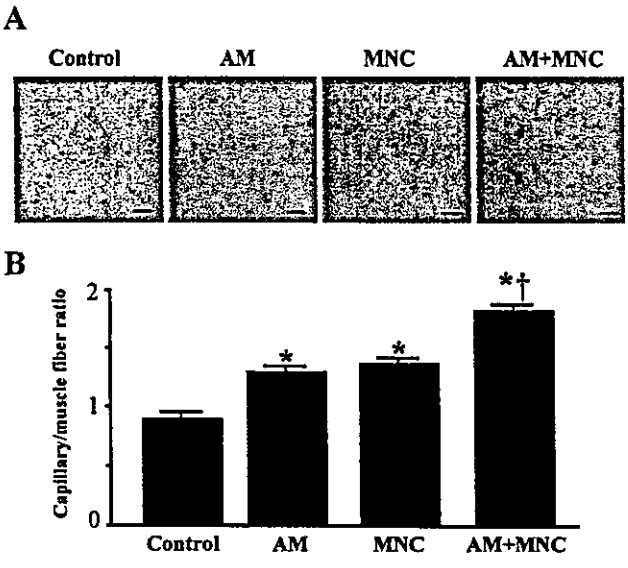

Figure 2. A, Representative photographs of alkaline phosphatase staining in ischemic hindlimb muscles. Capillary density in AM+MNC group was markedly higher than that in other groups. B, Quantitative analysis of capillary density in ischemic hindlimb muscles. Data are mean±SEM. *$P<0.01$ vs control; †$P<0.01$ vs AM and MNC. Scale bars: 50 μm.

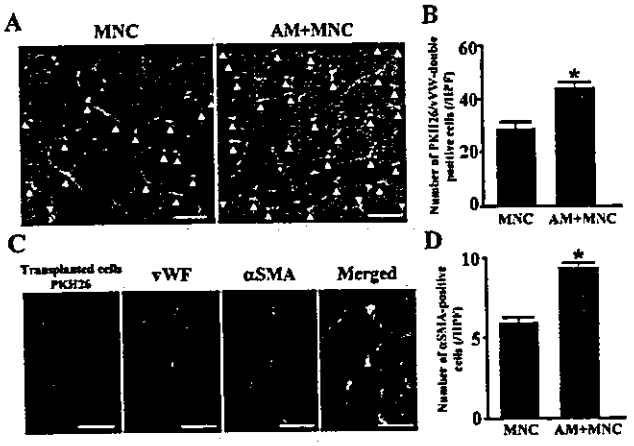

Figure 3. In vivo differentiation of transplanted MNCs. A, Representative photographs of MNC-derived vascular structures in MNC and AM+MNC groups. Red fluorescence (PKH26)–labeled MNCs were transplanted into ischemic thigh muscle. PKH26 (red)/vWF (blue) double-positive cells (pink, arrows) were frequently observed in AM+MNC group. B, Number of PKH26/vWF double-positive cells (MNC-derived endothelial cells) was significantly higher in AM+MNC group than in MNC group. C, Representative photographs of newly formed mature vessels in AM+MNC group. MNC-derived vascular structures often included α-SMA–positive cells (green). D, Number of α-SMA–positive cells in MNC-derived vessels was significantly higher in AM+MNC group than in MNC group. Data are mean±SEM. *$P<0.01$ vs MNC. Bars: 50 μm. HPF indicates high-power field.

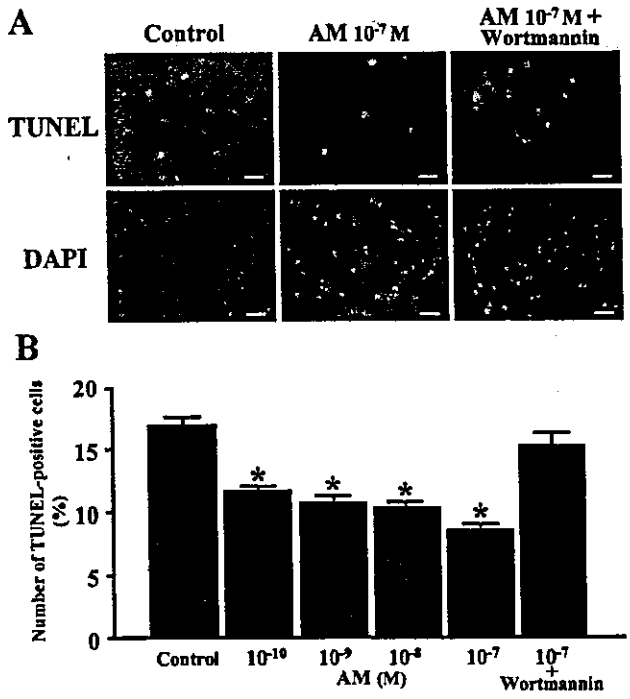

Figure 4. Apoptosis assay. A, Apoptosis of MNC was detected by TUNEL assay (green). Nuclei of MNC were stained with DAPI (blue). AM inhibited MNC apoptosis in serum-free medium. B, Quantitative analysis. AM decreased percentage of TUNEL-positive cells in dose-dependent manner. Pretreatment with wortmannin, a PI3K inhibitor, diminished antiapoptotic effect of AM. Data are mean±SEM. *$P<0.01$ vs control. Bars: 50 μm.

Antiapoptotic Effect of AM on MNCs

In vitro, serum starvation induced MNC apoptosis, as indicated by detection of TUNEL-positive cells (Figure 4A). When incubated in the presence of AM, the percentage of TUNEL-positive cells markedly decreased in a dose-dependent manner (Figure 4B). However, pretreatment with wortmannin, a PI3K inhibitor, diminished the antiapoptotic effect of AM. Similarly, in vivo, local administration of AM decreased TUNEL-positive MNC 24 hours after transplantation (data not shown).

Effect of AM on MNC Adhesiveness

The number of adherent MNCs on an HUVEC monolayer increased significantly in the presence of AM (10^{-7} mol/L) compared with control (Figures 5A and 5B). With pretreatment using tumor necrosis factor-α, AM also enhanced the adhesiveness of MNCs to HUVECs. AM significantly enhanced expression of ICAM-1 and VCAM-1 in HUVECs (Figure 5C).

Effect of AM on EPC Expansion

After 7-day culture of human MNCs, spindle-shaped or cobblestone-like adherent cells were observed (Figure 6A). Most of the adherent cells were double stained with DiI-acLDL and FITC-labeled lectin. These adherent cells expressed endothelial cell–specific markers: KDR, VE cadherin, and CD31 (Figure 6B). Thus, we identified the major population of the adherent cells as EPCs. Culture of MNCs with AM significantly increased the number of EPCs (Figure 6C). The effect of AM was equivalent to that of VEGF. Real-time PCR revealed that MNCs, EPCs, and HUVECs expressed mRNA of CRLR (Figure 6D). Expression of CRLR mRNA was highest in HUVECs, followed by EPCs and MNCs.

Effects of AM on Tube Formation and SMC Migration

Like VEGF, AM induced tube formation in HUVECs in vitro (Figure 7A). Blocking antibodies against KDR significantly inhibited VEGF-induced tube formation, whereas they did not suppress AM-induced tube formation (Figure 7B). AM did not significantly alter VEGF, basic fibroblast growth factor, or hepatocyte growth factor levels in conditioned medium of cultured MNCs or HUVECs (data not shown). AM significantly increased the number of migrated SMCs compared with control (Figures 7C and 7D). Pretreatment with wortmannin diminished the effect of AM on SMC migration.

Discussion

In the present study, we demonstrated in vivo that AM infusion or MNC transplantation alone induced angiogenesis in a rat model of hindlimb ischemia, the combination of AM infusion and MNC transplantation enhanced MNC-induced angiogenesis, and AM increased the number of MNC-derived vWF-positive cells and generated α-SMA–positive vascular structures. We also demonstrated in vitro that AM inhibited serum starvation–induced MNC apoptosis, promoted MNC adhesiveness to an HUVEC monolayer, increased the number of MNC-derived EPCs, and stimulated SMC migration.

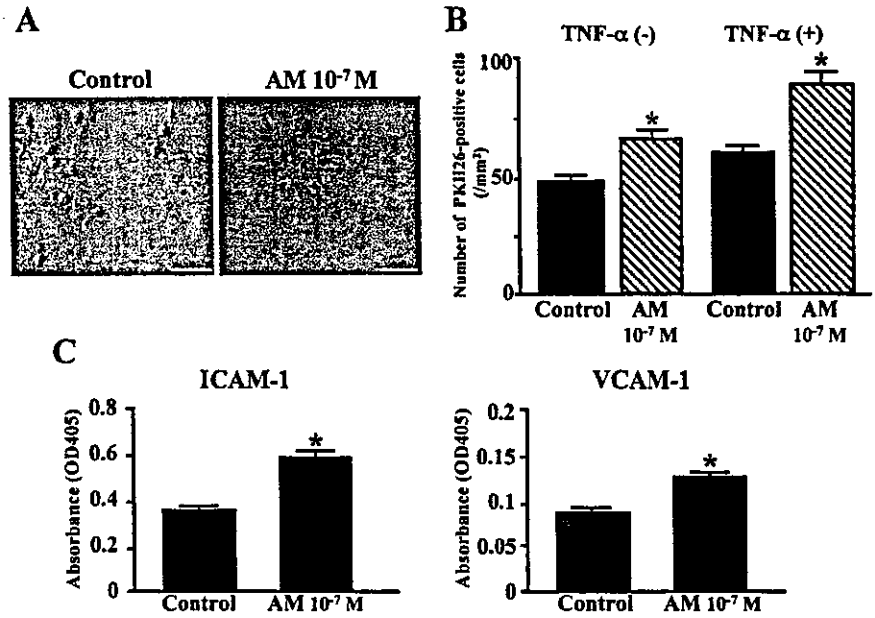

Figure 5. A and B, Adhesion assay. Representative photographs of red fluorescence–labeled MNC adhesion to HUVEC monolayer with and without AM (A). Quantitative analysis of MNC adhesion (B). Bars: 50 μm. C, Surface expression of ICAM-1 and VCAM-1 in HUVECs with or without AM. Data are mean±SEM. TNF indicates tumor necrosis factor. *$P<0.01$ vs control.

MNC transplantation causes therapeutic angiogenesis by supplying EPCs and multiple angiogenic cytokines such as VEGF.[3,4] The present study showed that local infusion of AM significantly increased blood perfusion and capillary density in ischemic hindlimb muscle. Furthermore, a combination of AM infusion and MNC transplantation significantly increased blood perfusion and capillary density of the ischemic hindlimb compared with MNC transplantation alone. AM has been shown to induce angiogenesis in vitro and in vivo through the PI3K/Akt pathway.[10,18] In the present study, AM-induced tube formation was not blocked by neutralizing antibodies against KDR. In addition, AM did not enhance VEGF secretion from MNCs and HUVECs. Thus, beneficial effects of combination therapy

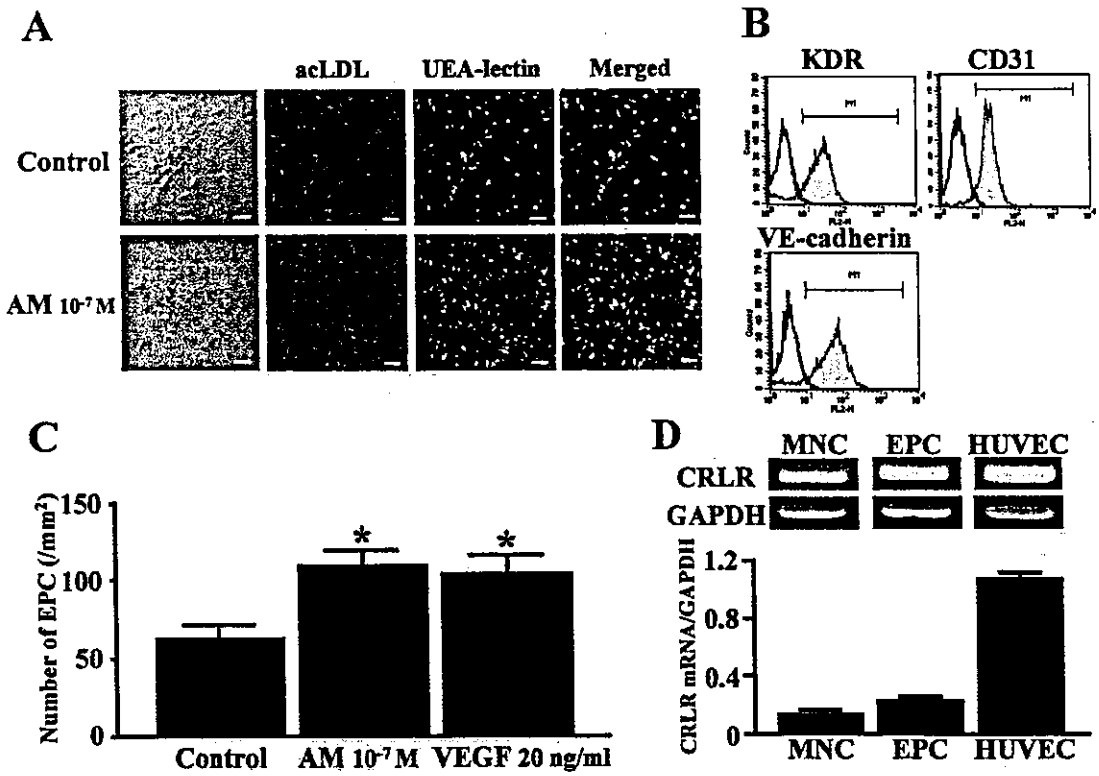

Figure 6. A through C, EPC culture assay. Cultured adherent cells took up DiI-acLDL (red) and FITC-labeled lectin (green) in same fields (A). Fluorescence-activated cell sorting analyses revealed that most adherent cells expressed KDR, VE cadherin, and CD31 (B). Culture of MNCs with AM significantly increased number of EPCs. Effect of AM was equivalent to that of VEGF (C). Data are mean±SEM. *$P<0.01$ vs control. Bars: 50 μm. D, Quantitative analysis of AM receptor (CRLR) mRNA expression in MNCs, EPCs, and HUVECs. UEA indicates ulex europaeus.

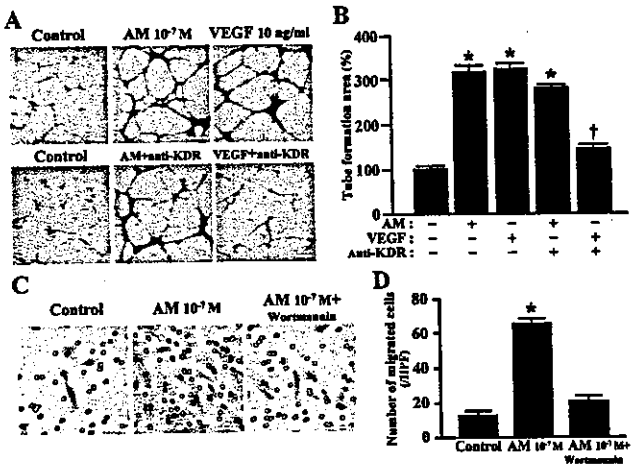

Figure 7. A and B, Matrigel assay. Representative photographs of tube formation (A). Quantitative analysis of tube formation area (B). Data are mean±SEM. *P<0.01 vs control; †P<0.01 vs VEGF. Bars: 20 μm. C and D, Migration assay. Representative photographs of migrated SMCs (C). Quantitative analyses of SMC migration (D). Data are mean±SEM. *P<0.01 vs control. Bars: 50 μm.

with AM and MNCs may be attributable in part to the angiogenic properties of AM itself.

An earlier study has shown that transplanted MNCs disappear from ischemic muscle 7 days after transplantation.[19] We demonstrated that apoptosis of MNCs occurred in ischemic muscle 24 hours after MNC transplantation. These results raise the possibility that the angiogenic potency of MNC transplantation is attenuated by MNC apoptosis. In the present study, AM inhibited apoptosis of MNCs in vitro and in vivo, and the antiapoptotic effect of AM was suppressed by wortmannin, a PI3K inhibitor. These findings suggest that AM prolongs MNC survival through the PI3K/Akt pathway and thereby enhances neovascularization in ischemic tissue.

In the present study, AM promoted adhesiveness of MNCs to an HUVEC monolayer. AM significantly enhanced expression of ICAM-1 and VCAM-1 in HUVECs, both of which facilitate adhesion of MNCs to endothelial cells.[20] These findings suggest that AM increases MNC adhesiveness to endothelial cells via activation of adhesion molecules. A recent study has shown that MNC adhesiveness to endothelial cells is indispensable for MNC differentiation into endothelial lineage.[21] Thus, it is possible that AM infusion enhances the angiogenic potency of MNCs at least in part through promotion of adhesion of MNC to host vascular endothelial cells.

VEGF has been shown to increase the number of EPCs in vitro and in vivo, resulting in angiogenesis and vasculogenesis.[13,22] The present study showed that MNCs and EPCs expressed CRLR, a receptor of AM. In vitro, AM increased the number of MNC-derived EPCs that expressed VE cadherin, KDR, and CD31. The effect of AM on EPC expansion was equivalent to that of VEGF. In vivo, AM infusion increased the number of MNC-derived vWF-positive cells, although incorporation of these cells in the capillaries may be due in part to incorporation of hematopoietic cells. These findings suggest that AM may accelerate MNC differentiation into endothelial lineage.

SMC is essential for the generation of functional and mature blood vessels.[23] We demonstrated in vivo that local infusion of AM increased the number of α-SMA–positive cells (SMCs) in MNC-derived vascular structures. In vitro, AM enhanced SMC migration, which was inhibited by wortmannin, a PI3K inhibitor. Recent studies using homozygous AM knockout mice have suggested that AM is indispensable for vascular morphogenesis.[6,7] When these findings are taken together, it is possible that AM contributes to vessel maturation through enhancement of SMC migration via the PI3K/Akt-dependent pathway.

Currently, a new therapeutic approach to augment the efficacy of MNC transplantation is awaited for the treatment of severe peripheral vascular disease. The present study demonstrated that local infusion of AM enhanced the angiogenic potency of MNC transplantation. In the present study, AM inhibited MNC apoptosis and increased the total number of engrafted cells in ischemic tissue, although this study did not show the effect of AM on specific cell populations of MNCs. In addition, AM promoted cell proliferation, migration, and differentiation. We have already demonstrated the safety of AM infusion in patients with congestive heart failure.[24] Thus, combination therapy with AM infusion and MNC transplantation may be a novel and promising therapeutic strategy for the treatment of severe peripheral vascular disease.

Conclusions

A combination of AM infusion and MNC transplantation caused significantly greater improvement in hindlimb ischemia than MNC transplantation alone. This effect may be mediated in part by the angiogenic potency of AM itself and the beneficial effects of AM on the survival, adhesion, and differentiation of transplanted MNCs.

Acknowledgments

This work was supported by the research grant for cardiovascular disease (16C-6) from the Ministry of Health, Labor and Welfare, Industrial Technology Research Grant Program in '03 from New Energy and Industrial Technology Development Organization (NEDO) of Japan, Health and Labor Sciences Research Grants-genome 005, the Mochida Memorial Foundation for Medical and Pharmaceutical Research, and the Promotion of Fundamental Studies in Health Science of the Organization for Pharmaceutical Safety and Research (OPSR) of Japan.

References

1. Belch JJ, Topol EJ, Agnelli G, et al. Critical issues in peripheral arterial disease detection and management: a call to action. *Arch Intern Med.* 2003;163:884–892.
2. Asahara T, Masuda H, Takahashi T, et al. Bone marrow origin of endothelial progenitor cells responsible for postnatal vasculogenesis in physiological and pathological neovascularization. *Circ Res.* 1999;85:221–228.
3. Shintani S, Murohara T, Ikeda H, et al. Augmentation of postnatal neovascularization with autologous bone marrow transplantation. *Circulation.* 2001;103:897–903.
4. Tateishi-Yuyama E, Matsubara H, Murohara T, et al. Therapeutic angiogenesis for patients with limb ischaemia by autologous transplantation of bone-marrow cells: a pilot study and a randomised controlled trial. *Lancet.* 2002;360:427–435.

5. Kitamura K, Kangawa K, Kawamoto M, et al. Adrenomedullin: a novel hypotensive peptide isolated from human pheochromocytoma. *Biochem Biophys Res Commun.* 1993;192:553–560.
6. Shindo T, Kurihara Y, Nishimatsu H, et al. Vascular abnormalities and elevated blood pressure in mice lacking adrenomedullin gene. *Circulation.* 2001;104:1964–1971.
7. Caron KM, Smithies O. Extreme hydrops fetalis and cardiovascular abnormalities in mice lacking a functional adrenomedullin gene. *Proc Natl Acad Sci U S A.* 2001;98:615–619.
8. Iimuro S, Shindo T, Moriyama N, et al. Angiogenic effects of adrenomedullin in ischemia and tumor growth. *Circ Res.* 2004;95:415–423.
9. Kim W, Moon SO, Sung MJ, et al. Protective effect of adrenomedullin in mannitol-induced apoptosis. *Apoptosis.* 2002;7:527–535.
10. Miyashita K, Itoh H, Sawada N, et al. Adrenomedullin provokes endothelial Akt activation and promotes vascular regeneration both in vitro and in vivo. *FEBS Lett.* 2003;544:86–92.
11. Murohara T, Ikeda H, Duan J, et al. Transplanted cord blood-derived endothelial precursor cells augment postnatal neovascularization. *J Clin Invest.* 2000;105:1527–1536.
12. Okumura H, Nagaya N, Itoh T, et al. Adrenomedullin infusion attenuates myocardial ischemia/reperfusion injury through the phosphatidylinositol 3-kinase/Akt-dependent pathway. *Circulation.* 2004;109:242–248.
13. Iwaguro H, Yamaguchi J, Kalka C, et al. Endothelial progenitor cell vascular endothelial growth factor gene transfer for vascular regeneration. *Circulation.* 2002;105:732–738.
14. Byrne MF, Corcoran PA, Atherton JC, et al. Stimulation of adhesion molecule expression by Helicobacter pylori and increased neutrophil adhesion to human umbilical vein endothelial cells. *FEBS Lett.* 2002;532:411–414.
15. Asahara T, Murohara T, Sullivan A, et al. Isolation of putative progenitor endothelial cells for angiogenesis. *Science.* 1997;275:964–967.
16. Nagaya N, Kangawa K, Kanda M, et al. Hybrid cell-gene therapy for pulmonary hypertension based on phagocytosing action of endothelial progenitor cells. *Circulation.* 2003;108:889–895.
17. Miura S, Matsuo Y, Saku K. Transactivation of KDR/Flk-1 by the B2 receptor induces tube formation in human coronary endothelial cells. *Hypertension.* 2003;41:1118–1123.
18. Tokunaga N, Nagaya N, Shirai M, et al. Adrenomedullin gene transfer induces therapeutic angiogenesis in a rabbit model of chronic hindlimb ischemia: benefits of a novel nonviral vector, gelatin. *Circulation.* 2004;109:526–531.
19. Iba O, Matsubara H, Nozawa Y, et al. Angiogenesis by implantation of peripheral blood mononuclear cells and platelets into ischemic limbs. *Circulation.* 2002;106:2019–2025.
20. Peled A, Grabovsky V, Habler L, et al. The chemokine SDF-1 stimulates integrin-mediated arrest of CD34(+) cells on vascular endothelium under shear flow. *J Clin Invest.* 1999;104:1199–1211.
21. Fujiyama S, Amano K, Uehira K, et al. Bone marrow monocyte lineage cells adhere on injured endothelium in a monocyte chemoattractant protein-1-dependent manner and accelerate reendothelialization as endothelial progenitor cells. *Circ Res.* 2003;93:980–989.
22. Asahara T, Takahashi T, Masuda H, et al. VEGF contributes to postnatal neovascularization by mobilizing bone marrow-derived endothelial progenitor cells. *EMBO J.* 1999;18:3964–3972.
23. Rissanen TT, Markkanen JE, Gruchala M, et al. VEGF-D is the strongest angiogenic and lymphangiogenic effector among VEGFs delivered into skeletal muscle via adenoviruses. *Circ Res.* 2003;92:1098–1106.
24. Nagaya N, Satoh T, Nishikimi T, et al. Hemodynamic, renal, and hormonal effects of adrenomedullin infusion in patients with congestive heart failure. *Circulation.* 2000;101:498–503.

□ CASE REPORT □

Primary Hyperparathyroidism Presumably Caused by Chronic Parathyroiditis Manifesting from Hypocalcemia to Severe Hypercalcemia

Sumiko FURUTO-KATO, Shigeru MATSUKURA, Makoto OGATA, Nobuyuki AZUMA, Toshiaki MANABE*, Chohei SHIGENO**, Ryo ASATO***, Kiyoshi TANAKA****, Yasato KOMATSU***** and Kazuwa NAKAO*****

Abstract

A 67-year-old woman who presented with hypocalcemia compatible with idiopathic hypoparathyroidism gradually changed into a state of primary hyperparathyroidism. The left upper parathyroid gland, which was larger and harder than other glands, was resected. Despite the operation, hypercalcemia and high levels of intact PTH persisted. Six weeks later total parathyroidectomy was done to induce remission. The resected gland in the first operation had clusters of lymphoid follicles with germinal centers indicating a chronic autoimmune inflammation. This case suggests a transition from hypoparathyroidim to hyperparathyroidism associated with chronic parathyroiditis, possibly by a mechanism analogous to that observed in chronic thyroiditis. (Internal Medicine 44: 60–64, 2005)

Key words: hyperparathyroidism, chronic parathyroiditis, lymphoid follicles with germinal centers, hypercalcemia, hypocalcemia, Hashimoto's disease

Introduction

Primary hyperparathyroidism is generally caused by parathyroid adenoma, hyperplasia or occasionally carcinoma. The cause of hyperparathyroidism without the above lesions is sometimes difficult to identify. Regarding the pathology of the parathyroid gland, lymphoid follicles with germinal centers are rarely present in the parathyroid tissues. The presence of lymphoid follicles may indicate a chronic inflammatory process in the tissue. Bondeson et al (1) first reported two cases of chronic parathyroiditis associated with hyperparathyroidism. The possibility of hyperparathyroidism caused by autoimmunity in the parathyroid gland in the context of Graves' disease-like lymphoid infiltrate has been postulated. Since there was no evidence of underlying infections, a developmental anomaly, or drug reactions that could explain the inflammatory component, they suggested that an autoimmune process may have been involved in the pathogenesis (1). Chronic parathyroiditis itself has rarely been reported to date. Furthermore, cases manifesting severe hypocalcemia later changing to severe hypercalcemia associated with chronic parathyroiditis have not been reported to our knowledge. We report here a rare case of primary hyperparathyroidism which was presumably due to chronic parathyroiditis, which manifested from hypocalcemia to severe hypercalcemia.

Case Report

A 67-year-old woman saw a home doctor because of finger numbness in January 2000. She was referred to our hospital because plasma Ca levels were 6.4 mg/dl. When she visited our hospital on February 23, 2000, her plasma Ca and P levels were 7.2 mg/dl and 7.0 mg/dl, respectively. Plasma intact parathyroid hormone (PTH) was less than 9 pg/ml; the threshold of the assay. Her height was 159.2 cm, and her weight was 48.4 kg. Her blood pressure was 143/84 mmHg. In terms of family history her sister died of cerebral bleed-

From the Metabolism and Endocrinology Division of Internal Medicine, Kishiwada City Hospital, Osaka, *Department of Pathology, Kyoto University Graduate School of Medicine, Kyoto, **Department of Radiology, JT Kyoto Senbai Hospital, Kyoto, ***Department of Otolaryngology-Head and Neck Surgery, Kyoto University Graduate School of Medicine, Kyoto, ****Department of Nutrition, Kyoto Women University, Kyoto and *****Department of Medicine and Clinical Science, Kyoto University Graduate School of Medicine, Kyoto

Received for publication February 2, 2004; Accepted for publication August 17, 2004

Reprint requests should be addressed to Dr. Sumiko Furuto-Kato, the Metabolism and Endocrinology Division of Internal Medicine, Kishiwada City Hospital, 1001 Gakuhara-cho, Kishiwada, Osaka 596-8501

ing, and she had had lung tuberculosis at 10 years of age. Physical examination on admission showed Chvostek sign and Trousseau sign, although the finger numbness had already disappeared. Laboratory data on admission on March 23, 2000 are summarized in Table 1. The results of Ellsworth-Howard test were compatible with idiopathic hypoparathyroidism. Other basal levels of hormones, with the exception of PTH, were within normal limits. Treatment with 1α, 25-(OH) D_3 2 μg/day was initiated.

Table 1. Ca Related Data on First Admission

Plasma Ca	6.5 mg/dl (8.6–10.6)
Plasma P	6.9 mg/dl (2.5–4.8)
Plasma Mg	1.9 mg/dl (1.5–2.8)
Ionized Ca	1.68 mEq/*l* (2.41–2.71)
24h urine Ca	0.03 g
24h urine Mg	0.05 g
Intact-PTH	13 pg/ml (10–65)
HS-PTH	200 pg/ml (160–520)
C-PTH	0.2 ng/ml (<0.5)
1.25-$(OH)_2$ Vitamin D	45.7 pg/ml (20–60)

( ): normal range.

Plasma Ca and intact PTH gradually increased. The clinical course is shown in Fig. 1. Treatment with 1α, 25-$(OH)_2$ D_3 was slowly tapered, then terminated. On November 13, 2000, plasma Ca and also intact PTH levels continued to increase without any treatment. In March 2001, both plasma Ca and intact PTH were above the normal upper limits. According to these state of parathyroid function, the clinical diagnosis was changed to primary hyperparathyroidism. Plasma Ca and intact PTH still increased slowly and consistently over the next several months, and six months after the diagnosis of primary hyperparathyroidism, an acute increase in plasma Ca levels occurred, peaking from 14.7 mg/dl to 16.5 mg/dl in September 2001 (Fig. 1). The patient suffered from severe fatigue, appetite loss and body weight loss of 9 kg, compatible with parathyroid crisis. A series of tests including an ultrasound echogram, 99mTc-MIBI/I-123 subtraction scintigraphy, magnetic resonance imaging (MRI), and computed tomography (CT) of the neck and the chest could not provide any information regarding localization of the causative lesions. Plasma PTH-related protein (PTHrP)

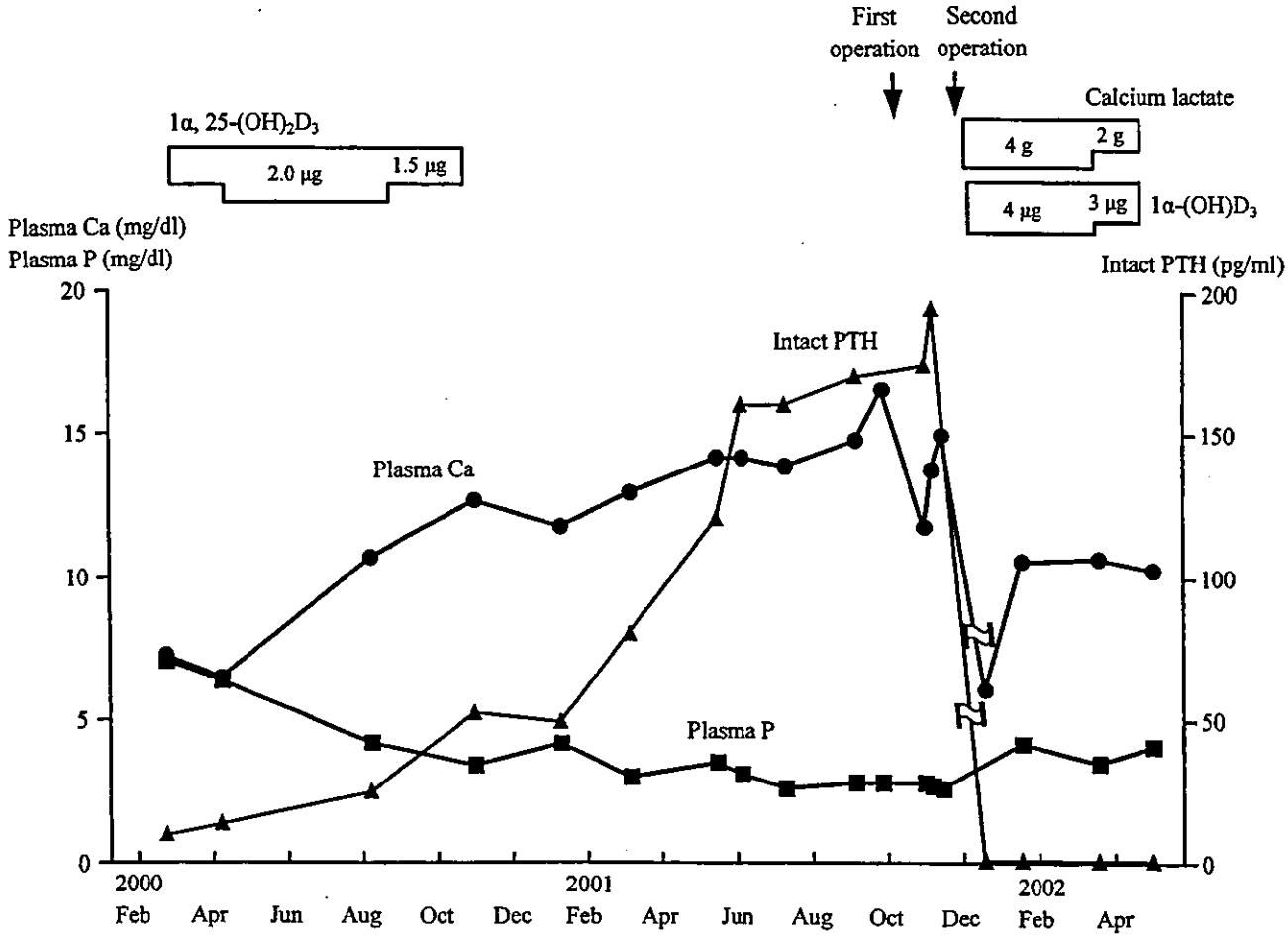

Figure 1. Clinical course of the patient.

Figure 2. Pathology of left superior parathyroid gland extirpated at the first operation demonstrating lymphoid follicles containing germinal centers.

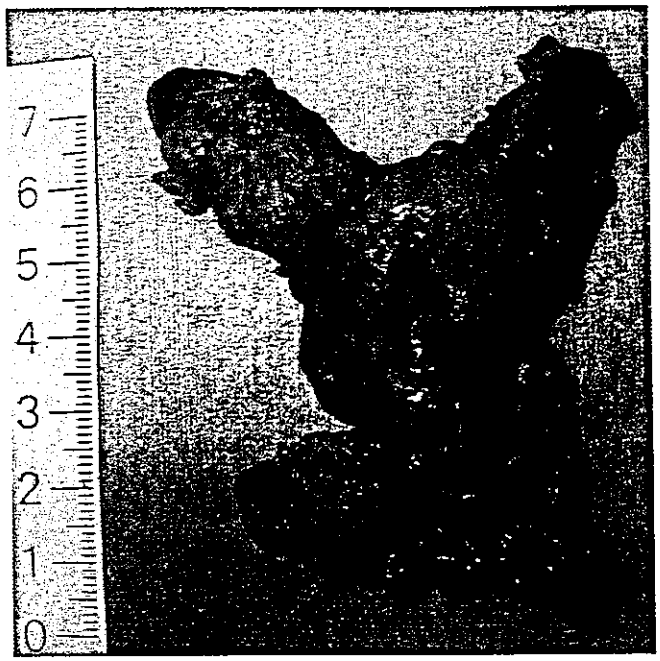

Figure 3. Resected specimens of the thyroid and fat tissue in the neck and superior thoracic region.

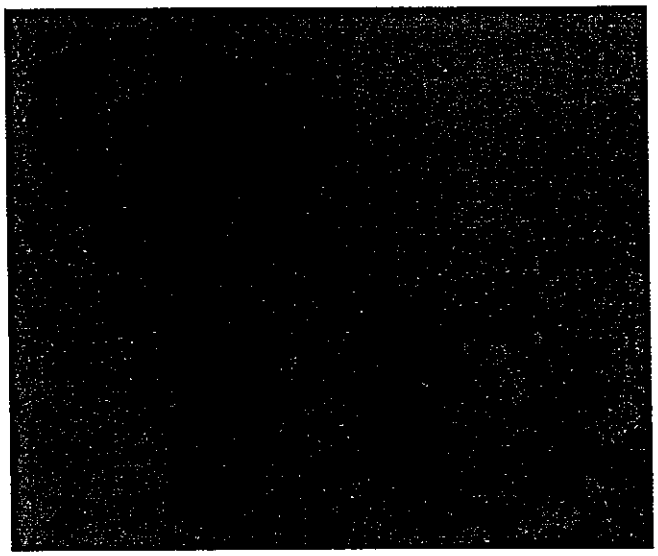

Figure 4. Pathology of the atrophic parathyroid gland resected at the second operation.

was within normal ranges. Antibodies against parathyroid gland and calcium-sensing receptor were not measured in the present study.

A parathyroidectomy was done on October 29, 2001. The left upper parathyroid gland, which was larger and harder than the other glands, was resected. Intrapoerative frozen section showed that it was compatible with the tumorous change. However, final detailed histological examination revealed that the resected gland was histologically almost normal and had infiltration of scattered lymphocytes and clusters of lymphoid follicles with germinal centers, indicating a chronic autoimmune inflammation (Fig. 2). Unfortunately, remission was not obtained after the operation. Venous sampling of the neck and the chest for intact PTH was performed. The levels of intact PTH were higher near the superior vena cava than the other regions. From this result, reoperation was elected.

After obtaining the informed consent, on December 7, 2001, total thyroidectomy and paratracheal neck-upper thoracic dissection (Fig. 3) were performed. After the operation, plasma Ca decreased and intact PTH was not detected: below the assay threshold. At present this state continues up, and 1α, 25-$(OH)_2D_3$ and thyroxine are given for replacement. With regard to the histology of the parathyroid glands, examinations of 4 mm slices identified the two additional parathyroid glands, that is, 1.8×0.7 mm in the tissue around the thyroid gland and 5 mm diameter in the paratracheal region. The former was atrophic (Fig. 4), and the latter was normal without any tumorous change and histologically there was focal infiltration of lymphcytes. Immunohistochemical staining for PTH was weakly positive in approximately 5% of the cells within the parathyroid gland resected at the first operation but the intensity of staining was weaker than that generally observed for normal parathyroid glands. Other glands resected at the second operation had been completely sliced thin, and thus no block was available for staining.

Discussion

The patient had clinical manifestations featuring a drastic change from hypocalcemia to hypercalcemia with pathological findings of lymphoid follicles with germinal centers in

the parathyroid gland but no evidence of commonly observed parathyroid adenoma, hyperplasia or carcinoma. Spontaneous remission due to sudden hemorrhage or infarction of parathyroid adenomas was reported in several cases of primary hyperparathyroidism (2, 3). This can be confirmed by findings of degenerative or necrotic tissues with hemosiderin deposits. Such rare cases are considered to be different from our case since there was neither hemorrhagic nor infarctive trace in the present study.

The pathological findings observed seem to simply lead us to the conclusion that the complicated clinical course could be explained by a mechanism associated with chronic parathyroiditis similar to that of Hashimoto's disease. Hashimoto reported patients with diffuse goiter and clarified the four histological characteristics: diffuse lymphocytic infiltration, formation of lymphoid follicles, destruction of epithelial cells, and proliferation of fibrous tissue (4). The term "Hashimoto's disease" or "Hashimoto thyroiditis" is used to refer not only to goitrous thyroiditis but also chronic thyroiditis or autoimmune thyroiditis including atrophic and nongoitrous thyroiditis. Thyroid function of this disease is variable, from hypothyroidism or euthyroidism to hyperthyroidism. There are some case reports in which the clinical manifestations change as a result of transition between chronic thyroiditis and Graves' disease (5–16). Graves' disease is also classified among autoimmune organ-specific diseases characterized by lymphocytic infiltration of the thyroid and circulating antibodies directed to thyroid-stimulating hormone (TSH) receptors including thyroid-stimulating antibodies. Some patients with primary hypothyroidism subsequently develop hyperthyroidism (5–13). Several factors are considered to explain the changes of thyroid function: disappearance or decrease in titer of a blocking type of TSH receptor antibodies (7–9, 11–13) and emergence or increase in titer of a stimulating-type of TSH receptor antibodies (6–10, 12, 13). Although antibodies against the parathyroid gland were not studied in this case, there was the possibility that such parathyroid-stimulating and/or -blocking antibodies might be involved. Immunohistochemical staining for PTH was weakly positive in lymphoid follicles in the parathyroid gland of this case. However the results of immunohistochemical staining for PTH do not reveal the state of function of the parathyroid glands, whether they are hypofunctional or hyperfunctional. Negative or weak staining is caused by hormone deficiency or by hypersecretion. For example, the vasopressin content in the posterior lobe can be evaluated using magnetic resonance (MR) imaging. On MR T1-weighted images, the posterior lobe is demonstrated as a characteristic hyperintense signal under normal conditions (17), and the signal intensity of the posterior lobe is thought to reflect the content of neurosecretory granules containing vasopressin. The hyperintense signal of the posterior lobe of the pituitary gland is absent in diabetes inspidus on MR T1-weighted imaging, in which vasopressin-deficient hyposecretion occurs. In contrast, the vasopressin content in the posterior lobe is also decreased in patients with uncontrolled diabetes mellitus, which was thought to be caused by persistent vasopressin hypersecretion (18).

Chronic parathyroiditis is rarely studied. In two extensive studies of parathyroid glands from 800 autopsies, only a single case of chronic parathyroiditis was found (19, 20). Hyperplastic parathyroiditis was also reported in a necropsy case, the function of which was unknown (21). Chronic parathyroiditis was also observed in a few cases of hypoparathyroidism (22, 23).

Thus far five cases of isolated hyperplastic parathyroiditis presenting with hyperparathyroidism have been reported. Two cases of chronic parathyroiditis associated with parathyroid hyperplasia and hyperparathyroidism are described by Bondeson et al (1). One case was a 62-year-old male whose serum calcium continually increased to 11.2 mg/dl (normal range 8.8–10.4 mg/dl). The patient became normocalcemic the day after parathyroidectomy, and serum calcium remained normal at follow-up after 4 years. The removed parathyroid glands contained lymphoid follicles with germinal centers. At the operation four enlarged parathyroid glands were identified. The three larger parathyroid glands were removed while the smallest one was left intact. The other case was a 53-year-old male whose serum calcium was increased to 10.8 mg/dl. Three enlarged parathyroid glands were removed while the smallest one, considered to be normal-sized, was left intact. This patient also became normocalcemic the day after the operation, and serum calcium remained normal at follow-up after 3 years. A third case of hyperparathyroidism associated with parathyroiditis coexisting with brachial-cleft cysts was reported (24). A 57-year-old man, whose calcium levels ranged from 13.52 to 13.60 mg/dl (normal range, 8.4–9.6 mg/dl) and whose PTH was 79.0 pg/ml (normal range, 0–55 pg/ml), had both enlarged inferior parathyroid glands removed. Both glands had similar features, including lymphoid tissue organized into follicles (some of which were replete with germinal centers), and numerous plasma cells (24). The fourth case of hyperparathyroidism associated with chronic parathyroiditis occurred in a multiple endocrine neoplasia type 1 (MEN-1) patient (25), and the fifth case remained hypercalcemic after removal of one parathyroid gland with lymphoid infiltration with germinal centers and one gland normal in microscopic appearance; the other glands were not investigated. In this case PTH was elevated to 164 pg/ml (normal range 10 to 55). Six months postoperatively serum calcium was 11.76 mg/dl and PTH was 90 pg/ml (26). All five cases presented clinically as primary hyperparathyroidism. The clinical course of our case is considered to have initially started as hypofunction, as in Hashimoto's disease, then to gradually have changed to hyperfunction as in Graves' disease, similar to autoimmune abnormalities often observed in the thyroid gland (5–13). Further similar case reports are required to analyze the details of the pathogenic mechanism of the parathyroid dysfunction associated chronic parathyroiditis.

In conclusion, we reported a case of hyperparathyroidism which initially presented with hypocalcemia associated with

lymphoid follicles with germinal centers in one parathyroid gland and later one atrophic and one normal parathyroid gland pathologically.

References

1) Bondeson AG, Bondeson L, Ljungberg O. Chronic parathyroiditis associated with parathyroid hyperplasia and hyperparathyroidism. Am J Surg Pathol **8**: 211–215, 1984.
2) Kovacs KA, Gay JD. Remission of primary hyperparathyroidism due to spontaneous infarction of a parathyroid adenoma: Case report and review of the literature. Medicine (Baltimore) **77**: 398–402, 1998.
3) Natsui K, Tanaka K, Suda M, Yasoda A, Yonemitsu S, Nakao K. Spontaneous remission of primary hyperparathyroidism due to hemorrhagic infarction in the parathyroid adenoma. Intern Med **35**: 646–649, 1996.
4) Hashimoto H. Zur Kenntniss der lymphomatösen Veränderung der Sc hilddrüse (Struma lymphomatosa). Arch Klin Chir **97**: 219–248, 1912 (in German).
5) Yamasaki H, Takeda K, Nakauchi Y, Suehiro T, Hashimoto K. Hypothyroidism preceding hyperthyroidism in patient with continuously positive stimulating antibody. Internal Medicine **34** (4): 247–250, 1995.
6) Kasagi K, Konishi J, Iida Y, Mori T, Torizuka K. Changes in thyroid-stimulating and TSH binding inhibitory activities in a patient who developed hyperthyroidism due to Graves' disease following primary hypothyroidism. Clin Endocrinol **25**: 519–525, 1986.
7) Takeda K, Takamatsu J, Kasagi K, et al. Development of hyperthyroidism following primary hypothyroidism following primary hypothyroidism: a case report with changes in thyroid-related autoantibodies. Clin Endocrinol **28**: 341–344, 1988.
8) Cho BY, Skong YK, Lee HK, Koh CS, Min HK. Graves' hyperthyroidism following primary hypothyroidism: sequential changes in various activities of thyrotropin receptor antibodies following primary hypothytoidism. Acta Endocrinol (Copenh.) **120**: 447–450, 1989.
9) Takasu N, Yamada T, Sato A, et al. Graves' disease following hypothyroidism due to Hashimoto's diseasse: Sudies of eight cases. Clin Endocrinol (Oxf.) **33**: 687–698, 1990.
10) Tamai H, Kasagi K, Mizuno O, et al. Thyroid-stimulating antibody and thyrotropin-binding inhibitory immunoglobulin activity in hypothyroid patients who subsequently developed thyrotoxicosis. Acta Endocrinol **122**: 499–504, 1990.
11) Kraiem Z, Baron E, Kahana L, Sadeh O, Sheinfeld M. Changes in stimulating and blocking TSH receptor antibodies in a patient undergoing three cycles of transition from hypo to hyper-thyroidism and back to hypothyroidism. Clin Endocrinol (Oxf.) **36**: 211–214, 1992.
12) Kasagi K, Hidaka A, Endo K, et al. Fluctuating thyroid function depending on the balance between stimulating and blocking types of TSH receptor antibodies: a case report. Thyroid **3**: 315–318, 1993.
13) Miyauchi A, Amino N, Tamaki H, Kuma H. Coexistence of thyroid-stimulating and thyroid-blocking antibodies in a patient with Graves' disease who had transient hypothyroidism. Am J Med **85**: 418–420, 1998.
14) Tamaki H, Amino N, Aozasa M, Mori M, Tanizawa O, Miyai K. Serial changes in thyroid-stimulating antibody and thyrotropin binding inhibitory immunoglobulins at the time of postpartum occurrence of thyrotoxicosis in Graves' disease. J Clin Endocrinol Metab **65**: 324–330, 1987.
15) Kasagi K, Tamai H, Morita T, et al. Role of thyrotopin receptor antibodies in the development of hyperthyroidism: follow-up studies on nine patients with Graves' disease. J Clin Endocrinol Metab **68**: 1189–1194, 1989.
16) Tamai H, Kasagi K, Morita T, et al. Thyroid response, especially to thyrotropin-binding inhibitory immunoglobulins, in euthyroid relatives of patients with Graves' disease: a clinical follow-up. J Clin Endocrinol Metb **71**: 210–215, 1990.
17) Fujisawa I. Magnetic resonance imaging of the hypothalamic-neurohypophyseal system. J Neuroendocrinol **16**: 297–302, 2004.
18) Fujisawa I, Murakami N, Furuto-Kato S, Araki N, Konishi J. Plasma and neurohypophyseal content of vasopressin in diabetes mellitus. J Clin Endocrinol Metab **81**: 2805–2809, 1996.
19) Seemann N. Untersuchungen zur haufigkeit der lymphozytaren parathyreiditis. Dtsch Med Wochenschr **92**: 106–108, 1967 (in German).
20) Thiele J, Ries P, Georgii A. Spezielle und funktionelle pathomorphologie der epitelkorperchen in einem unausgewahlten obduktionsgut (589 sektionen). Virchows Arch A Pathol Anat Histol **367**: 195–208, 1975 (in German).
21) Boyce BF, Doherty VR, Mortimer G. Hyperplastic parathyroiditis a new autoimmune disease? J Clin Pathol **35**: 812–814, 1982.
22) Kossling FK, Emmrich P. Demonstration eines falles von kindlichem morbus Addison mit hypoparathyreoidismus. Verh Dtsch Ges Pathol **55**: 155–160, 1971 (in German).
23) Van de Casseye M, Gepts W. Case report: Primary (autoimmune?) parathyroiditis. Virchows Arch A Pathol Anat **361**: 257–261, 1973.
24) Chetty R, Forder MD. Parathyroiditis associated with hyperparathyroidism and branchial cysts. Am J Clin Pathol **96**: 348–350, 1991.
25) Sinha SN, McArdle JP, Shepherd JJ. Hyperparathyroidism with chronic parathyroiditis in a multiple endocrine neoplasia patient. Aust NZ J Surg **63**: 981–982, 1993.
26) Vaizey CJ, Ali M, Gilbert JM. Chronic parathyroiditis associated with primary hyperplastic hyperparathyroidism. J R Soc Med **90**: 336–337, 1997.

Osteoporosis International
With other metabolic bone diseases

10.1007/s00198-004-1786-z

Original Article

Decreased bone mineral density at the distal radius, but not at the lumbar spine or the femoral neck, in Japanese type 2 diabetic patients

T. Majima[1], Y. Komatsu[2] ✉, T. Yamada[1], Y. Koike[1], M. Shigemoto[1], C. Takagi[1], I. Hatanaka[1] and K. Nakao[2]

(1) Department of Endocrinology and Metabolism, Rakuwakai Otowa Hospital, Kyoto, Japan

(2) Department of Medicine and Clinical Science, Kyoto University Graduate School of Medicine, 54 Shogoin Kawahara-cho Sakyo-ku, 606-8507 Kyoto, Japan

✉ **Y. Komatsu**
Email: komatsuy@barium.rirc.kyoto-u.ac.jp
Phone: +81-75-7513168
Fax: +81-75-7719452

Received: 1 June 2004 **Accepted:** 18 August 2004 **Published online:** 19 November 2004

Abstract The purpose of this study is to assess the association between type 2 diabetes and bone mineral density. This study included 145 Japanese patients (64 men and 81 women) with type 2 diabetes and 95 non-diabetic control subjects (41 men and 54 women) of similar age. We measured bone mineral density (BMD) at the sites with different cortical/cancellous bone ratio (lumbar spine, femoral neck, and distal radius) using dual-energy X-ray absorptiometry. BMD and Z score at the distal radius were significantly lower in type 2 diabetic patients than those in control subjects, and in type 2 diabetic patients, the Z score at the distal radius was lower than that at their own lumbar spine and femoral neck. In type 2 diabetic patients, negative correlation between BMD and the mean HbA1c during the previous 2 years was found significantly at the distal radius in both genders and at the femoral neck in women. These results indicate the selective cortical bone loss in type 2 diabetes and suggest the importance of also determining BMD at the radius and keeping good metabolic control to prevent bone loss in type 2 diabetic patients.

Keywords Bone mineral density - Distal radius - Insulin levels - Type 2 diabetes mellitus

Introduction

Decreased bone mineral density (BMD) is an established complication of type 1 diabetes [*1*, *2*]. However, contradictory results have been reported in BMD of type 2 diabetic patients thus far:

several studies have shown that BMDs at the lumbar spine and the femoral neck were either unaltered [2, 3, 4, 5, 6, 7, 8, 9, 10] or increased [3, 6, 7, 8, 10, 11, 12, 13], rarely decreased [4, 10, 14] and that BMD at the distal radius was decreased [1, 15], not different [3, 6], or increased [3]. These complicated results suggest that examining BMDs at different sites may reveal different results, especially in type 2 diabetic patients. Therefore, it seems insufficient to measure the BMD of type 2 diabetic patients at a single site. Thus, in this study, we measured the BMD of Japanese type 2 diabetic men and women at the sites with different cortical/cancellous bone ratio: lumbar spine, femoral neck, and distal radius, using dual-energy X-ray absorptiometry (DXA).

Some papers reported that BMD was decreased more severely in the poorly controlled type 2 diabetic patients [1, 14]. On the other hand, some papers reported that insulin was an important factor in maintaining BMD [16, 17, 18, 19]. Japanese type 2 diabetic patients have the racial feature that they are mildly obese, with decreased capacity of insulin secretion, from a relatively early stage of the disease [20, 21]. It is, therefore, of interest to assess the relationship of BMD with BMI, the metabolic control and the capacity of insulin secretion in Japanese type 2 diabetic patients.

Subjects and methods

Subjects

One hundred and forty-five Japanese patients with type 2 diabetes (64 men and 81 women) were included in this study (Table 1). They were randomly selected from patients attending the diabetes clinic of Rakuwakai Otowa Hospital during the period between December 2002 and April 2003. Type 2 diabetes was diagnosed on the basis of an abnormal glucose tolerance test result, classic symptoms, and laboratory findings. The inclusion criteria for this study were type 2 diabetes diagnosed at the age of over 30 years and duration of diabetes for more than 2 years. Among 64 type 2 diabetic men, 20 were treated by diet only, 25 with oral medication, and 19 with insulin, and among 81 type 2 diabetic women, 25 were treated by diet only, 22 with oral medication and 34 with insulin. No patient had a history of ketosis and no patient had diabetic retinopathy, nephropathy or peripheral neuropathy.

Table 1 Means ± SD of the variables assessed in examined subjects (N.D. not done)

Variable	Men		Women	
	Diabetic patients	Control subjects	Diabetic patients	Control subjects
	(*n*=64)	(*n*=41)	(*n*=81)	(*n*=54)
Age (years)	62.8±12.0^{NS}	62.9±11.3	66.6±11.4^{NS}	66.1±11.8
BMI (kg/m^2)	23.6±3.6^{NS}	23.1±2.5	23.6±4.6^{NS}	23.2±3.1
Creatinine (mg/dl)	0.75±0.2^{NS}	0.72±0.2	0.63±0.2^{NS}	0.63±0.2
Calcium (mg/dl)	9.2±0.3^{NS}	9.3±0.3	9.2±0.4^{NS}	9.3±0.5
Phosphate (mg/dl)	3.3±0.7^{NS}	3.4±0.6	3.5±0.7^{NS}	3.4±0.6
Urinary NTx/Cre	38.8±11.7	N.D.	44.9±18.6^{NS}	50.6±19.3

(nmol BCE/mmol Cre)				
ALP (IU/l)	229.0±57.7	N.D.	245.8±66.5[NS]	234.4±66.5
IRI (μU/ml)	7.0±3.6	N.D.	6.4±3.6	N.D.
Urinary CPR (μg/day)	62.8±42.3	N.D.	45.2±32.6	N.D.
FPG (mg/dl)	153.7±46.6[†]	90.8±5.3	155.5±62.4[†]	91.2±5.5
Mean HbA1c (%)	7.8±1.6	N.D.	7.6±1.6	N.D.

P values for comparisons between patients with type 2 diabetes mellitus and control subjects: [NS]$P>0.05$, [†]$P<0.01$

The non-diabetic healthy control subjects were 41 Japanese men and 54 women (Table 1) and were selected from patients attending the clinic of Rakuwakai Otowa Hospital for their annual medical checkups during the same period. The diabetic patients and the control subjects were similar with regard to physical activity.

All subjects were interviewed by the doctor or nurse and underwent laboratory blood tests. We excluded the subjects who had a history of any fractures and other diseases (liver disease, renal dysfunction, malignancy, hyperthyroidism, hyperparathyroidism, hypercorticoidism, or hypogonadism) and those who had a history of taking medications (active vitamin D3, bisphosphonates, calcitonin injection, estrogens, steroids, thyroid hormone, diuretics, heparin or anticonvulsants) that could influence bone metabolism. All the subjects were subjected to plain X-ray (anteroposterior and lateral views) for the lumbar spine, and patients with scoliosis, compression fractures or ectopic calcifications that could interfere with the bone mineral results were excluded. No subjects were smokers or alcoholics. All subjects gave informed consent.

BMD measurements

BMD was measured at the lumbar spine (L2–L4), the femoral neck, and the distal radius, by DXA (Hologic QDR 4500c, Hologic, Waltham, Mass., USA). To eliminate technical variation, the same operator measured all the subjects. Values of BMD at the lumbar spine were presented as the mean of those at L2–L4. T scores and Z scores were calculated on the basis of the normal reference values of the age- and gender-matched Japanese group provided by the DXA system manufacturer.

Biochemical measurements

Serum calcium, phosphate, creatinine and fasting plasma glucose (FPG) were measured by routine methods. In the type 2 diabetic patients, plasma HbA1c was measured by the latex agglutination method (Fuji Rebio, Tokyo, Japan) and was presented as the mean of several values during the last 2 years before BMD measurement. In diabetic patients treated by diet only or with oral medications (i.e., 45 diabetic men and 47 diabetic women), serum immunoreactive insulin (IRI) was measured by immunoradiometric assay (BML, Kawagoe, Japan) after overnight fasting, and urinary connecting peptide immunoreactivity (CPR) was measured by radioimmunoassay (BML) of the 24-h urine samples collected and stored at –20°C. As markers of bone formation and resorption, serum alkaline phosphatase (ALP) and urinary N-terminal telopeptide of type I collagen normalized by creatinine (NTx/Cre) were measured in diabetic patients and control women. ALP was measured by the routine method (*P*-nitrophenyl-phosphate substrate method).

Urinary NTx in the second urine samples in the morning was measured by enzyme-linked immunosorbent assay (BML).

Statistical analysis

Data were analyzed by *t*-test between two group differences, by one-way factorial ANOVA and Fisher's protected least significant difference (PLSD) method among three group differences, and by Pearson's correlation test for examining correlation. Statistics were calculated with Statview version 4.0 (Abacus Concepts, Berkeley, Calif., USA). A P value <0.05 was considered as statistically significant.

Results

Table 1 shows a comparison between type 2 diabetic patients and control subjects. There was no significant difference between the two groups in age, BMI and the biochemical parameters except FPG. Among the three diabetic subgroups treated in different ways: diet only, oral medication, and insulin, there was also no significant difference in age, BMI and the mean HbA1c as well as the number of each subgroup (data not shown).

Table 2 and Fig. 1A show a comparison of BMD, T score and Z score between type 2 diabetic patients and control subjects. BMD, T score and Z score at the distal radius were significantly lower in type 2 diabetic patients than in control subjects but were not different at the lumbar spine and the femoral neck, although the Z score at the lumbar spine was significantly higher in type 2 diabetic women. Among the three diabetic subgroups with different treatments, there was no significant difference in BMD, T score and Z score at the three sites (data not shown).

Table 2 BMD, T score and Z score at the lumbar spine, the femoral neck and the distal radius in type 2 diabetic patients and control subjects. Values are means ± SD

Parameter	Men		Women	
	Diabetic patients	Control subjects	Diabetic patients	Control subjects
Lumbar spine				
BMD (g/cm^2)	0.972±0.176^{NS}	0.975±0.108	0.861±0.193^{NS}	0.831±0.162
T score (SD)	–0.640±1.481^{NS}	–0.614±0.905	–1.259±1.618^{NS}	–1.509±1.360
Z score (SD)	0.120±1.005^{NS}	0.096±0.595	0.533±1.175†	0.025±0.979
Femoral neck				
BMD (g/cm^2)	0.759±0.137^{NS}	0.767±0.108	0.620±0.153^{NS}	0.660±0.118
T score (SD)	0.820±1.083^{NS}	0.755±0.723	–1.533±1.408^{NS}	–1.167±1.079
Z score (SD)	0.118±1.049^{NS}	0.087±0.787	0.087±1.320^{NS}	0.152±1.075
Distal radius				
BMD (g/cm^2)	0.665±0.092*	0.721±0.080	0.493±0.109†	0.547±0.095
T score (SD)	–1.287±1.311*	–0.492±1.144	–3.321±2.131†	–2.257±1.858

Z score (SD)	−0.610±1.101†	0.044±1.014	−0.397±1.583*	0.175±1.224

P-values for comparisons between type 2 diabetic patients and control subjects: $^{NS}P>0.05$, $^{*}P<0.05$, $^{\dagger}P<0.01$

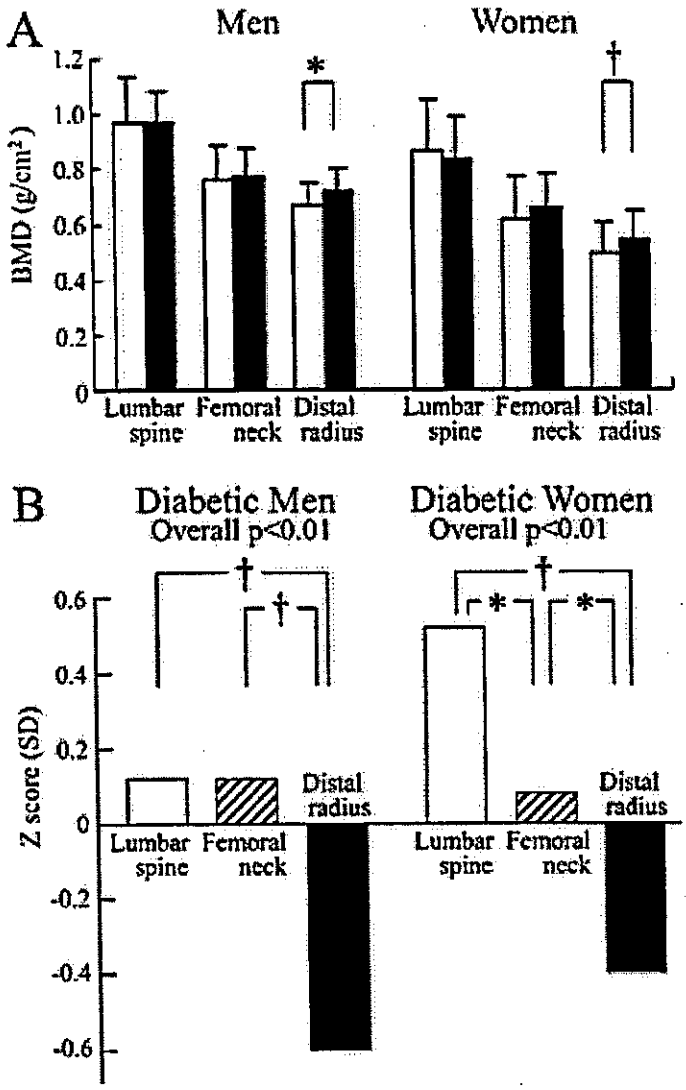

Fig. 1 A Comparison of BMDs at the lumbar spine, the femoral neck and the distal radius between patients with type 2 diabetes mellitus (*open columns*) and control subjects (*closed columns*). Each column represents the mean ± SD. *$P<0.05$, † $P<0.01$. **B** Comparison of Z scores at the lumbar spine (*open columns*), the femoral neck (*shaded columns*) and the distal radius (*closed columns*) in patients with type 2 diabetes mellitus. Each column represents the mean value. *$P<0.05$, † $P<0.01$.

Figure 1B shows a comparison of Z scores at different sites in type 2 diabetic patients, analyzed by one-way factorial ANOVA and Fisher's PLSD test. Z score at the distal radius was significantly lower than those at the lumbar spine and the femoral neck in both men and women, and at the lumbar spine it was significantly higher than that at the femoral neck in women, but not in men.

Table 3 shows correlations of BMD with age, BMI and the biochemical parameters in type 2

diabetic patients. However, correlations of BMD with IRI and urinary CPR were calculated only in type 2 diabetic patients treated by diet only or with oral medications (i.e., 45 diabetic men and 47 diabetic women) because those two parameters were not measured in our insulin-treated patients, as mentioned above. BMDs at the three sites in both genders were associated negatively with age and positively with BMI, except BMD at the distal radius in men with BMI (P=0.0754). Urinary NTx/Cr was negatively correlated with BMD at the lumbar spine in both genders, at the femoral neck in men, and at the distal radius in women. ALP was not correlated with BMD, except at the femoral neck in men. IRI was positively correlated with BMD at the lumbar spine in women, at the femoral neck in both genders, and at the distal radius in men. Urinary CPR was positively correlated with BMD at the femoral neck and the distal radius in both genders. FPG was not correlated with BMD at any site. The mean HbA1c was negatively correlated with BMD at the femoral neck in women and at the distal radius in both genders (Fig. 2D, E, F), and there was a tendency of negative correlation of the mean HbA1c with BMD at the lumbar spine and at the femoral neck in men (Fig. 2A, C).

Table 3 Correlations of BMD with age, BMI and the biochemical parameters in type 2 diabetic patients. Values are correlation coefficients. IRI immunoreactive insulin, CPR connecting peptide immunoreactivity, FPG fasting plasma glucose

Parameter	BMD					
	Men			Women		
	Lumbar spine	Femoral neck	Distal radius	Lumbar spine	Femoral neck	Distal radius
Age	–0.310*	–0.519†	–0.409†	–0.409†	–0.575†	–0.692†
BMI	0.375†	0.435†	0.224NS	0.365†	0.493†	0.438†
Creatinine	0.156NS	–0.019NS	–0.034NS	0.130NS	0.049NS	0.042NS
Calcium	0.047NS	0.051NS	0.200NS	0.107NS	0.005NS	0.267NS
Phosphate	0.051NS	–0.065NS	0.079NS	–0.158NS	–0.136NS	–0.166NS
Urinary NTx/Cre	–0.346†	–0.247*	–0.127NS	–0.303*	–0.215NS	–0.258*
ALP	–0.140NS	–0.325†	–0.073NS	–0.050NS	–0.137NS	–0.091NS
IRI	0.085NS	0.305*	0.304*	0.394†	0.382†	0.218NS
Urinary CPR	0.108NS	0.296*	0.314*	0.287NS	0.534†	0.488†
FPG	–0.069NS	–0.019NS	0.035NS	0.056NS	–0.137NS	–0.049NS
Mean HbA1c	–0.182NS	–0.240NS	–0.289*	–0.032NS	–0.314†	–0.219*

P values for correlations of BMD with age, BMI and the biochemical parameters in type 2 diabetic patients: $^{NS}P>0.05$, $^{*}P<0.05$, $^{\dagger}P<0.01$

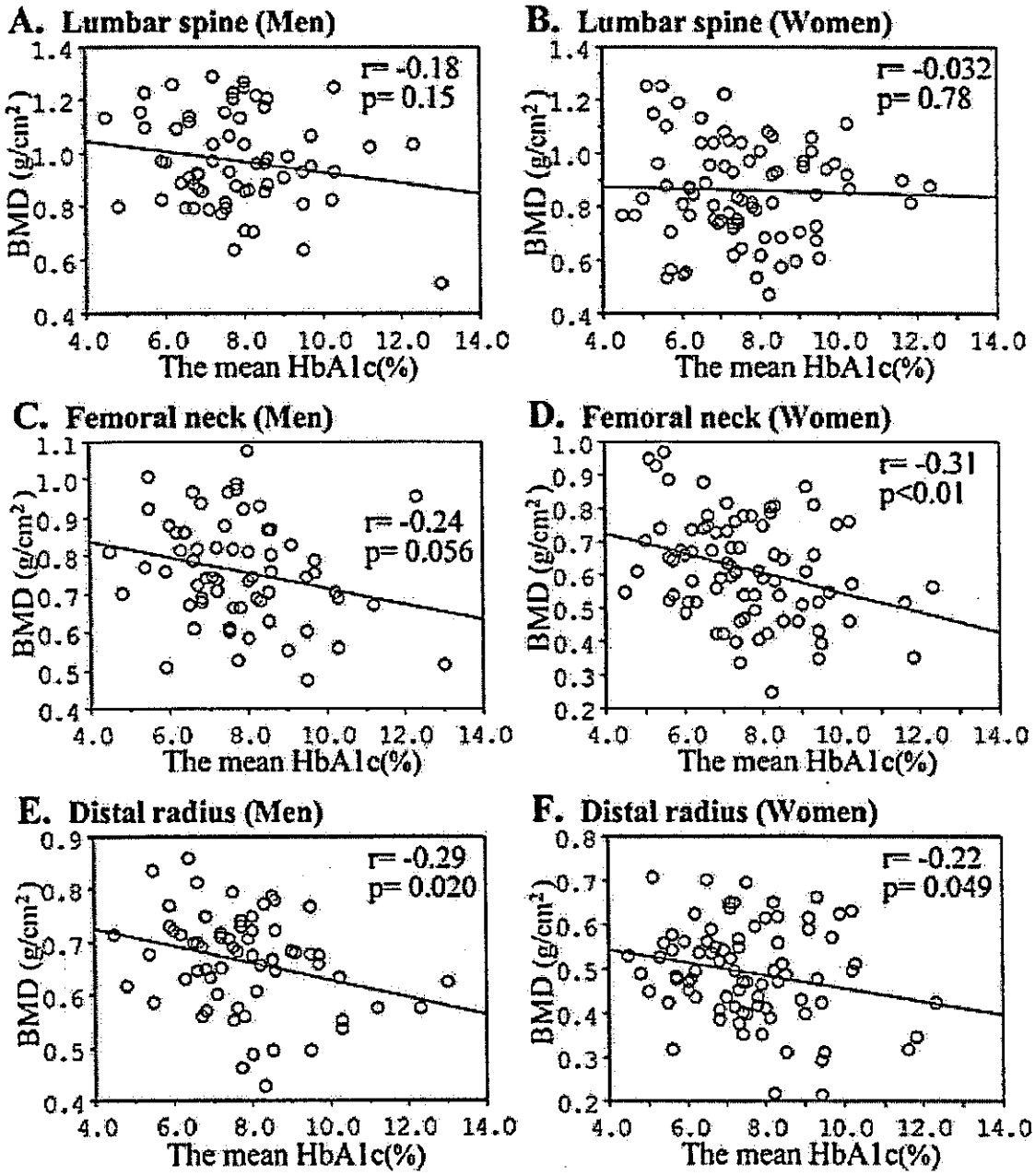

Fig. 2A–F Correlation between the mean HbA1c and BMD at the three sites: lumbar spine (**A, B**), femoral neck (**C, D**) and distal radius (**E, F**) in diabetic men (**A, C, E**) and diabetic women (**B, D, F**). For each figure the BMD measurements at each site were plotted against the mean HbA1c levels *The line* reflects the regression and *r* mean correlation coefficients and *P* values for correlations between the mean HbA1c and BMD at the three sites.

Discussion

Our study revealed that BMD of type 2 diabetic patients was significantly lower at the distal radius, but not different at the lumbar spine and the femoral neck, than that of control subjects. and our new finding was that the Z score was the lowest at the distal radius among the three sites (lumbar spine, femoral neck and distal radius) in type 2 diabetic patients. Our results showed that

the higher the cortical/cancellous bone ratio (distal radius >femoral neck >lumbar spine), the lower the Z-score became (lumbar spine >femoral neck >distal radius) in type 2 diabetic women. These results suggest that the rapid loss of cortical bone rather than cancellous bone may occur in type 2 diabetes.

Christensen and Svendsen also reported the difference in Z scores among the three sites (lumbar spine >femur total >distal radius) shown in the present study [6]. They examined the BMD of type 2 diabetic women by DXA, but they did not show the statistical significance among the three sites. Leite Duarte and da Silva [22] reported reduced cortical thickness of bone biopsy samples in type 2 diabetic patients. Those results are compatible with our results, suggesting a selective cortical bone loss in type 2 diabetes.

There seem to be many reasons why BMD and Z score at the distal radius were lower in Japanese type 2 diabetic patients in our study, although those at the lumbar spine and femoral neck were higher or not different. The results of the previous studies about BMD of type 2 diabetes were controversial [1, 2, 3, 4, 5, 6, 7, 8, 9, 10, 11, 12, 14, 15]. The different insulin levels in type 2 diabetic patients, high in newly onset cases, low in long-standing cases, might be one of the explanations for the contradictory results of the previous studies [3, 11, 18]. Many previous studies and our present study showed a positive correlation of insulin levels with BMDs [16, 17, 18, 19], because insulin has an anabolic effect on bone [23]. Moreover, Haffner and Bauer [16] and Stolk et al. [18] reported that there was a difference between the association of insulin level with BMD at the lumbar spine and at the femur. Also, our results revealed a difference in the association of insulin level with BMD at the three sites. These results might imply a different effect of insulin on cortical bone from cancellous bone. Therefore, Japanese type 2 diabetic patients with low insulin secretion may have the risk of losing cortical bone and have lower BMDs, especially at the distal radius.

The association between BMDs and insulin levels may be the result of the association between BMD and some other osteogenic factors related to insulin: amylin, estrogen, testosterone, and sex hormone-binding globulin (SHBG). Amylin, which is co-secreted with insulin by the pancreatic β cells in response to glucose load, inhibits bone resorption [24] and increases bone formation [24, 25, 26]. Sex steroids, including estrogen and testosterone, are correlated with insulin levels [7, 18, 27], inhibit bone resorption and increase BMD [28, 29]. Low SHBG levels are correlated with high insulin levels [27, 30] and lead to high sex hormone levels, causing increased BMD [17, 31]. In our study, BMI was strongly correlated with insulin levels, both in men and women with type 2 diabetes ($r=0.454$ $P=0.0018$, $r=0.467$ $P=0.0018$, respectively), as reported in the previous studies [3, 17]. Those insulin-related factors may have influenced bone metabolism and caused the difference in association of insulin levels with BMDs at the three sites in our study.

In the present study, the mean HbA1c was negatively correlated with BMD at the femoral neck in women and the distal radius in both genders, but not at the lumbar spine. Therefore, the association of the mean HbA1c with BMD in the present study seems to be different by the cortical/cancellous bone ratio. This difference may have caused the difference of Z score among the three sites in our study.

Higher BMD associated with poor metabolic control in type 2 diabetic patients [3, 6, 7, 8, 10, 11, 12, 13] could be explained by their hyperinsulinemia, as stated by Stolk et al. in their own study [18]. However, on the other hand, in Japanese type 2 diabetic patients their insulin secretion is not high enough to catch up with increased glucose levels [20, 21]. Therefore, poor metabolic control was not associated with hyperinsulinemia, and so did not lead to higher BMD in our study. Krakauer et al. [1] and Gregorio et al. [14] reported that BMD was decreased in the poorly

controlled type 2 diabetic patients and that it was increased by improving metabolic control. Some in vitro studies showed that exposure to high glucose impaired the activity of osteoblasts [32] and stimulated osteoclasts [33]. Those results are in agreement with our results, suggesting that metabolic control of type 2 diabetes is important in preventing bone loss as well as other complications.

Higher parathyroid hormone (PTH) secretion, in part by the negative calcium balance in type 2 diabetic patients, might be one of the reasons for the selective cortical bone loss in type 2 diabetes [14, 34]. Although we did not measure serum PTH, serum calcium was not different between the diabetic patients and the controls.

Whether the bone turnover of type 2 diabetes is higher or lower has not reached consensus yet [1, 5, 6, 7, 8, 12, 14, 22, 34, 35]. Some previous studies reported reduced bone formation in bone biopsy samples of type 2 diabetic patients [1, 22], and reduced osteocalcin in type 2 diabetic patients has been repeatedly reported [6, 7, 34]. Those results are interpreted to represent low bone formation in type 2 diabetes [1, 6, 7, 22, 34]. However, in contrast, ALP and bone type alkaline phosphatase (BAP), other bone formation markers, were reported to be elevated in type 2 diabetes in other previous studies [35, 36], as in our study. This is probably because maturation of osteoblasts is inhibited at the mineralization phase after ALP expression in type 2 diabetes [37]. Therefore, considering that in our study ALP was relatively higher and urinary NTx/Cre was relatively lower in type 2 diabetic women, we consider that type 2 diabetic women in our study had relatively a lower rate of bone turnover than controls. This lower rate of bone turnover may offset rapid bone loss with high bone turnover during perimenopausal period [1, 3, 6], especially at the lumbar spine. Therefore, type 2 diabetic women in the present study might not have lost bone at the lumbar spine, and so their BMD at the lumbar spine might have become higher than that of control women and also than their own BMDs at the other sites.

From these observations, it can be seen that cortical bone and cancellous bone could be differently affected by the conditions of type 2 diabetes, including insulin, glucose, BMI, sex steroids and PTH. However, further studies are needed to clarify these issues.

In conclusion, we found that BMD at the distal radius was significantly decreased in type 2 diabetic patients compared with controls and that Z score at the radius was significantly lower than that at their own lumbar spine and their own femoral neck in type 2 diabetic patients. In addition, we found negative correlation of the mean HbA1c during the previous 2 years with BMD at the femoral neck and the distal radius, but not at the lumbar spine, in type 2 diabetic patients. These results suggest a selective cortical bone loss in type 2 diabetes. Therefore, we conclude that it is important to determine BMD at the radius as well and that good metabolic control leads to prevention of bone loss in type 2 diabetic patients.

Acknowledgement This work is supported by grants from Research for the Future of the Japan Society for the Promotion of Science; the Japanese Ministry of Education, Sciences, Sports, and Culture; Smoking Research Foundation and Foundation for Growth Science.

References

1. Krakauer JC, McKenna MJ, Buderer NF, Rao DS, Whitehouse FW, Parfitt AM (1995) Bone loss and bone turnover in diabetes. Diabetes 44:775–782
ChemPort PubMed

2. Tuominen JT, Impivaara O, Puukka P, Ronnemaa T (1999) Bone mineral density in patients with type 1 and type 2 diabetes. Diabetes Care 22:1196–1200
ChemPort PubMed

3. Barrett-Connor E, Holbrook TL (1992) Sex differences in osteoporosis in older adults with non-insulin-dependent diabetes mellitus. JAMA 16:3333–3337
crossref

4. Wakasugi M, Wakao R, Tawata M, Gan N, Koizumi K, Onaya T (1993) Bone mineral density by dual energy X-ray absorptiometry in patients with non-insulin-dependent diabetes mellitus. Bone 14:29–33
crossref ChemPort PubMed

5. Sosa M, Dominquez M, Navarro MC, Segarra MC, Hernandez D, de Pablos P, Betancor P (1996) Bone mineral metabolism is normal in non-insulin-dependent diabetes mellitus. J Diabetes Complications 10:201–205
crossref ChemPort PubMed

6. Christensen JO, Svendsen OL (1999) Bone mineral in pre- and postmenopausal women with insulin-dependent and non-insulin-dependent diabetes mellitus. Osteoporos Int 10:307–311
SpringerLink ChemPort PubMed

7. el Miedany YM, el Gaafary S, el Baddini MA (1999) Osteoporosis in older adults with non-insulin-dependent diabetes mellitus: is it sex related? Clin Exp Rheumatol 17:561–567
PubMed

8. Isaia GC, Ardissone P, Di Stefano M, Ferrari D, Martina V, Porta M, Tagliabue M, Molinatti GM (1999) Bone metabolism in type 2 diabetes mellitus. Acta Diabetol 36:35–38
SpringerLink ChemPort PubMed

9. Bartos V, Jirkovska A, Kasalicky P, Smahelova A, Vondra K, Skibova J (2001) Osteopenia and osteoporosis in diabetic women over 40 years of age. Cas Lek Cesk 140:299–301
ChemPort PubMed

10. Sert M, Tetiker T, Kirim S, Soyupak S, Canataroglu A, Kocak M (2003) Type 2 diabetes mellitus and osteopenia: is there an association? Acta Diabetol 40:105–108
ChemPort PubMed

11. van Daele PL, Stolk RP, Burger H, Algra D, Grobbee DE, Hofman A, Birkenhager JC, Pols HA (1995) Bone density in non-insulin-dependent diabetes mellitus: the Rotterdam Study. Ann Intern Med 122:409–414
PubMed

12. Sahin G, Bagis S, Cimen OB, Ozisik S, Guler H, Erdogan C (2001) Lumbar and femoral bone mineral density in type 2 Turkish diabetic patients. Acta Medica (Hradec Kralove) 44:141–143

13. Akin O, Gol K, Akturk M, Erkaya S (2003) Evaluation of bone turnover in postmenopausal type 2 diabetic patients using biochemical markers and bone mineral density measurements. Gynecol Endocrinol 17:19–29
ChemPort PubMed